Seismic imaging of melt in a displaced Hawaiian plume

Catherine A. Rychert[1]*, Gabi Laske[2], Nicholas Harmon[1] and Peter M. Shearer[2]

The Hawaiian Islands are the classic example of hotspot volcanism: the island chain formed progressively as the Pacific plate moved across a fixed mantle plume[1]. However, some observations[2] are inconsistent with simple, vertical upwelling beneath a thermally defined plate and the nature of plume-plate interaction is debated. Here we use S-to-P seismic receiver functions, measured using a network of land and seafloor seismometers, to image the base of a melt-rich zone located 110 to 155 km beneath Hawaii. We find that this melt-rich zone is deepest 100 km west of Hawaii, implying that the plume impinges on the plate here and causes melting at greater depths in the mantle, rather than directly beneath the island. We infer that the plume either naturally upwells vertically beneath western Hawaii, or that it is instead deflected westwards by a compositionally depleted root that was generated beneath the island as it formed. The offset of the Hawaiian plume adds complexity to the classical model of a fixed plume that ascends vertically to the surface, and suggests that mantle melts beneath intraplate volcanoes may be guided by pre-existing structures beneath the islands.

Beneath Hawaii, the interaction of the plume with the overlying plate manifests a ∼1,000-km-wide bathymetric swell around the islands. Although a heated[3] or mechanically thinned[4] lithosphere could support the swell, the observed Hawaiian heat-flow anomaly is probably too small to be evidence for thinning[2]. Lithospheric thinning has been seismically imaged, although not beneath the region of active volcanism, but farther northwest along the island chain, again suggesting a model with greater complexity[4]. Alternatively, dynamic compensation[5] or a compositionally buoyant root[6–8] may provide better explanations. However, seismic imaging of plume impingement on the plate has proved challenging, including resolving the expected underlying pancake of hot material and its effect on the shape of the overriding plate.

Here we use S-to-P (Sp) receiver functions to image sharp seismic discontinuities beneath Hawaii. We use data from the plume–lithosphere undersea mantle experiment (PLUME)[9,10], which consisted of nearly 70 seafloor sites and 10 land stations, as well as permanent island stations (Fig. 1). An extended multitaper deconvolution is carried out followed by migration and stacking[11]. The velocity model used for migration corrects for elevations and uses the crustal velocity model from P-to-S (Ps) imaging[12] and mantle velocities from surface waves[10] (also see Supplementary Information). The discontinuities are indicated using blue for negative-polarity phases (shear velocity decreases with depth) and red for positive-polarity phases (shear velocity increases with depth; Fig. 2).

A strong negative-polarity lithosphere–asthenosphere boundary (LAB) phase is imaged at 93 ± 10 km west of the main island and 75 ± 10 km beneath the eastern edge of the island (blue
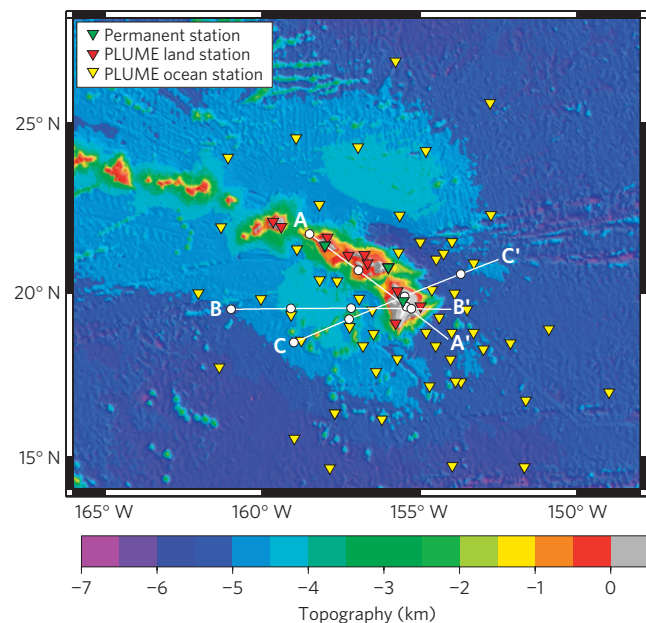

Figure 1 | Map of the Hawaiian study region. Coloured surface shows bathymetry and topography. Inverted triangles indicate seismic stations: permanent land (green), PLUME Carnegie Institution of Washington land (red) and PLUME ocean (yellow)[9,10]. White lines show cross-sections in Fig. 2. Circles along cross-sections are for scale, every 200 km, as in Fig. 2.

phase, Fig. 2). Although the phase is subtly shallower closer to the island axis, the variation is within our error bars for depth. Furthermore, a strong positive-polarity discontinuity is imaged throughout the region at greater depths, ∼110–155 $\pm$ 10 km (red phase labelled 'onset of melting', Fig. 2). The discontinuity deepens from 110 ± 10 km in well-resolved regions surrounding the islands to 155 ± 10 km in a narrow ∼200-km-wide zone just west of the main island of Hawaii, extending north beneath the island chain. The Moho discontinuity (shallowest red phase, Fig. 2) is imaged at depths generally consistent with those from Ps imaging beneath the islands[12]. A positive phase near ∼50 km depth surrounding the islands is far too deep to be the oceanic Moho and rather represents an imaging artefact (see Supplementary Information).

The negative-polarity phase at ∼75–93 km depth agrees with general predictions for the thickness of the thermally defined 100-million-year-old (100-Myr-old) lithosphere[13]. The deeper measurements also agree with a previous Sp study near the main island (95 km depth below sea level) from waveforms stacked

[1]Ocean and Earth Science, National Oceanography Centre Southampton, University of Southampton, European Way, Southampton SO14 3EZ, UK, [2]Institute of Geophysics and Planetary Physics, Scripps Institution of Oceanography, University of California, San Diego, 9500 Gilman Drive, La Jolla, California 92093-0225, USA. *e-mail: c.rychert@soton.ac.uk
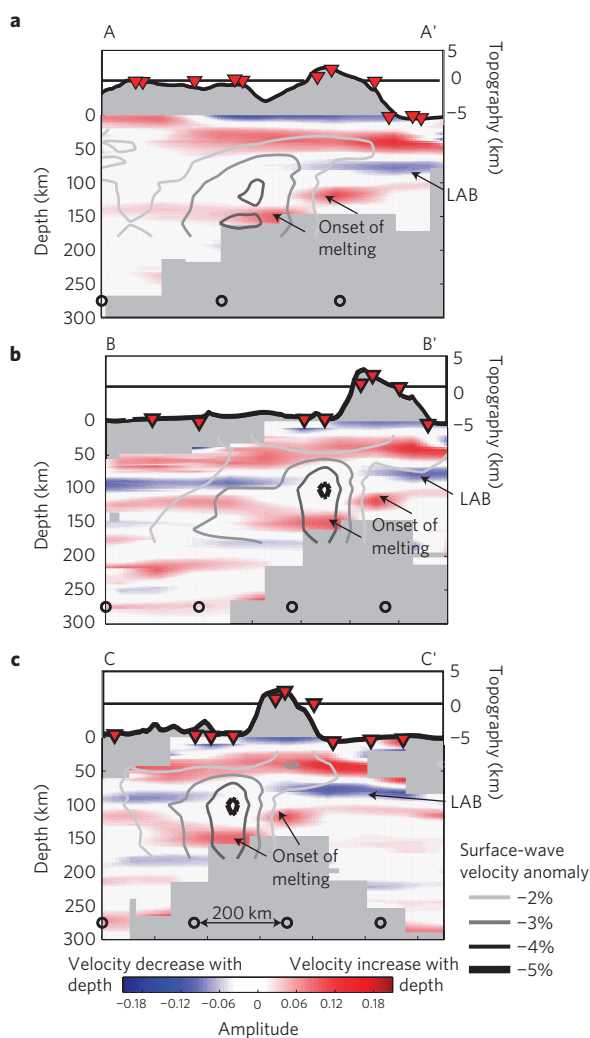
Figure 2 | Cross-sections through the migrated receiver functions compared with shear velocity anomaly contours from surface-wave analysis. Colour indicates polarity of receiver function discontinuities, positive for shear-wave velocity increases with depth (red) and negative for decreases (blue). Contours show surface-wave shear velocity anomalies (slower with increasing darkness) from −2% (grey) to −5% (thick black)[10]. Open circles at 275 km depth correspond to those in Fig. 1, spaced at 200 km. Bathymetry is plotted at the top of each panel, with exaggeration. Inverted red triangles show station locations. Note that the colour axis is subtly asymmetric. Regions with insufficient data are shaded grey (see Supplementary Information).

in wide hotspot-track-perpendicular bins[4]. The slightly shallower LAB on the eastern edge of the main island (~75 km) agrees well with estimates from nearby SS precursors (76–81 ± 7 km depth beneath sea level)[14]. Although the slope on the LAB is not well resolved, one possible interpretation is a westward-dipping LAB. The presence and sharpness of the positive-polarity phase at ~110–155 ± 10 km depth is supported by previous detection of a positive discontinuity at 130–140 km depth in a single location beneath western Hawaii with Ps receiver functions, which are sensitive only to the sharpest velocity gradients[15].

Modelling indicates that the LAB is probably strong and sharp, defined by a mechanism other than thermal gradients alone[14,16–18] (see Supplementary Information). The positive-polarity discontinuity at 110–155 ± 10 km depth similarly represents a strong velocity increase with depth that is again too sharp to be explained by vertical thermal gradients (see Supplementary Information). This

is especially true within plume conduits where thermal gradients are expected to be quite diffuse and also true beneath the plume pancake region[6] (see Supplementary Information). One possible mechanism includes hydration supplied by the plume, which may decrease mantle velocities and cause sharp velocity gradients in depth[19]. However, in plume environments, where temperatures are predicted to be supersolidus, hydration partitions into the melt, increasing seismic velocity where melting has occurred in the past, that is, in the 110–155 km depth range, which is inconsistent with observations[10]. Therefore, a small amount of partial melting is probably retained beneath the LAB in quantities sufficient for detection by seismic waves, that is, about ~1% (refs 11,20). The strong velocity increase in depth at 110–155 km depth probably represents a sharp transition from a melt-rich zone to the deeper mantle where seismically detectable melt is absent, that is, the onset of partial melting in the mantle.

Here the phase interpreted as the depth of melting migrates to ~125 km throughout most of the imaged region. However, ~100 km west of the island of Hawaii, the phase seems much deeper, at ~155 km depth (Fig. 2). These depths, 125 km and 155 km, correspond to predictions for the onset of melting at potential temperatures of ~1,450 and ~1,550 °C, implying a thermal anomaly of ~100 °C locally or ~200 °C from ambient mantle (see Supplementary Fig. S3). In other words, the deeper onset of melting ~100 km west of the island of Hawaii is likely to be the location of a strong thermal plume anomaly, highlighting the location of plume impingement on the lithosphere. Indeed, our geophysical estimates for both potential temperature (1,550 °C) and depth of melting (155 km) are in excellent agreement with independent geochemical estimates for the plume temperature and associated melting depth (1,500–1,600 °C, 150–180 km)[21]. This interpretation is also supported by surface-wave analysis, which resolves a low-velocity anomaly west of Hawaii, markedly, in the exact location where we observe a deepened solidus (area of deeper red phases compared with black contours in Fig. 2)[10]. Surface waves provide good tomographic resolution in this depth range, whereas receiver functions constrain both velocity gradient depth and sharpness, and therefore the associated mechanism of the anomaly.

Several other observations are similarly consistent with plume impingement 100 km west of the island. Ocean bathymetry is much shallower on the western side of the islands than on the east (Fig. 1), suggesting an additional source of buoyancy to the west, such as a plume. Also, the Loa volcanoes (southwestern edge of young Hawaiian Islands) are more isotopically enriched than the Kea trend (northeastern edge of young Hawaiian Islands), which could result from a plume conduit that is more proximal to the Loa trend[22], in line with our model. Furthermore, the retained partial melting inferred from our observations may add additional support for the Hawaiian Swell through melt buoyancy without requiring a large plume flux[5], a large thermal anomaly[2], or significant thinning of the lithosphere[3].

Plume impingement 100 km west of the island of Hawaii is at odds with the notion of a simple vertically upwelling plume geometry. At first glance, off-axis plume impingement seems to imply that the plume has moved, which may indeed be possible[23]. However, recent plume movement in the past ~0.5 Myr since the formation of the island of Hawaii, after ~47 Myr of plume fixity, based on the age progression of the Hawaiian island chain, is probably too coincidental. Instead, interaction with convection currents may cause non-vertical plume ascent[24]. In this case, the plume may naturally approach the surface from the west. Indeed, receiver functions image a thinned transition zone ~200 km southwest of Hawaii[15] and SS waveforms were used to argue for ponded plume material beneath the transition zone several degrees west of Hawaii[25].
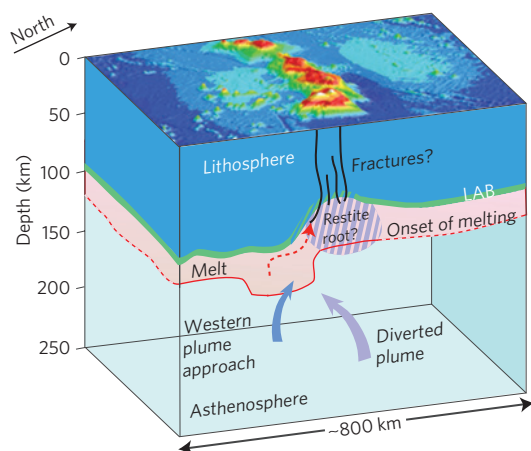
Figure 3 | Interpretative schematic of plume–plate interaction. A thermal plume impinges on the LAB (green line) 100 km west of Hawaii, depressing the onset of melting (red). The plume either naturally approaches from the west (blue arrow) or is diverted (purple dashed arrow) by a restite root (purple oval). Layered regions include the lithosphere (dark blue layer), the melt-rich zone (pink) and the asthenosphere (cyan and pink layers). Melt travels towards the island of Hawaii (red dashed arrow), directed by a gently sloping permeability barrier at the LAB and/or pre-existing lithospheric fractures (back lines) caused by volcanic loading[27].

Alternatively, the plume may be located beneath the island of Hawaii at depths greater than ~155 km, as suggested by seismic body-wave tomography[9], but deflected westwards at shallower depths owing to a hot, but resistive, body that has formed beneath the Hawaiian Islands[6] (Fig. 3). A restite root beneath the main island is a logical byproduct of the large increase in magma flux that has occurred over the past ~5 Myr, creating the Hawaiian Islands[26]. The direction of deflection may be related to topography on the root and/or pre-existing deeper plume directionality. Although the plume heats the resistive body beneath the main island today, the melt-rich zone directly beneath the main island remains shallow, <110 km depth, owing to compositional depletion. Combined heat and compositional depletion may make the root itself difficult to detect seismically.

In both the westward approach and the deflected plume model, melt must find its way from the region of plume impingement to the islands where volcanism is observed. Melt pathways may be significantly different from those of solid mantle flow. A gently sloping permeability boundary at the LAB and/or pre-existing fractures related to volcanic loading and lithospheric flexure[27] may promote melt transport towards the surface volcanoes. A sloped LAB may have formed in the past when the plume initiated volcanism beneath the island. Indeed, a sloped interface towards the axis of volcanism in both temperature and viscosity profiles exists in models that include a restite root[6].

The existence of seismically imageable partial melt in the asthenosphere is debated. It is often evoked to explain the magnitude of slow seismic velocity anomalies[10,28] and seismic imaging of strong, sharp velocity decreases with depth at the LAB[11,14,17,18]. However, observations of strong velocity increases in the 60–155 km depth range, that is, the base of the melt zone, are relatively rare. Therefore, it is often assumed that either melt percentage gradually decreases with depth, or that melt retention is insufficient over a broad enough depth range to be seismically imageable. In the latter case another mechanism such as hydration[19,29] or some combination of temperature and grain size[30] must be employed to explain strong, sharp LAB observations. However, our observations suggest that beneath locations such as hotspots[14], rifts[11] and ridges[28] high melt retention may exist between a lithosphere

and asthenosphere permeability boundary and the onset of melting, sharply dropping off at deeper depths. Such imaging facilitates global seismic comparisons of mantle potential temperatures and melting dynamics. For instance, the melting depth within the Hawaiian plume conduit (~155 km) is much deeper than that beneath the Afar Rift (~75 km) where volcanism is driven primarily by decompression melting[11].

Methods

We used events located at epicentral distances of 55°–80° from the stations. The orientations of the horizontal components of the PLUME ocean bottom seismometers (OBSs) were determined during post-deployment processing of the data using the polarization of teleseismic surface waves (both Rayleigh and Love waves; Supplementary Table S1). For each event, waveforms were rotated into theoretical P and SV components and then handpicked (see Supplementary Information). Each SV waveform was deconvolved from P using an extended multitaper method[11] and filtered from 0.05 to 0.14 Hz. Unstable outputs were eliminated. Receiver function polarity was flipped to agree with polarities from Ps imaging. The waveforms were then migrated onto a grid with 3/4° bins (Supplementary Fig. S1). Data were weighted according to signal-to-noise ratio. Bins with less than three waveforms were discarded and the grid was smoothed according to Fresnel zone width. Bins without data and bins in which amplitudes are not significant according to 95% confidence limits are shaded grey. Reported depths are with respect to sea level. We carried out one-dimensional forward modelling with synthetic seismograms to constrain the velocity gradient interpreted as the onset of melting 100 km west of the island of Hawaii (Supplementary Fig. S2). A vertical depth section in the data was chosen centred on the location where the positive phase interpreted as the onset of melting is deepest. We also carried out synthetic seismogram modelling to explore the effect of water and sediment layers on OBSs and to investigate the accuracy of Moho depth estimates (see Supplementary Information). We used a simple two-dimensional geodynamic model of a plume to calculate expected geotherms and melt production and retention. We then translated these results to seismic shear velocity to explore the mechanisms that may explain our seismic observations.

References

1. Morgan, W. J. Convection plumes in lower mantle. *Nature* **230,** 42–43 (1971).
2. VonHerzen, R., Cordery, M., Detrick, R. & Fang, C. Heat flow and the thermal origin of hot spot swells: The Hawaiian Swell revisited. *J. Geophys. Res.* **94,** 13783–13799 (1989).
3. Detrick, R. & Crough, S. Island subsidence, hot spots, and lithospheric thinning. *J. Geophys. Res.* **83,** 1236–1244 (1978).
4. Li, X. Q., Kind, R., Yuan, X. H., Wolbern, I. & Hanka, W. Rejuvenation of the lithosphere by the Hawaiian plume. *Nature* **427,** 827–829 (2004).
5. Sleep, N. H. Hotspots and mantle plumes—some phenomenology. *J. Geophys. Res.* **95,** 6715–6736 (1990).
6. Yamamoto, M. & Morgan, J. P. North Arch volcanic fields near Hawaii are evidence favouring the restite-root hypothesis for the origin of hotspot swells. *Terra Nova* **21,** 452–466 (2009).
7. Hall, P. S. & Kincaid, C. Melting, dehydration, and the dynamics of off-axis plume-ridge interaction. *Geochem. Geophys. Geosys.* **4,** 8510 (2003).
8. Jordan, T. H. in *The Mantle Sample: Inclusions in Kimberlites and Other Volcanics* Vol. 2 (eds Boyd, F. R. & Meyer, H. O. A.) 1–14 (AGU, 1979).
9. Wolfe, C. J. *et al.* Mantle shear-wave velocity structure beneath the Hawaiian Hot Spot. *Science* **326,** 1388–1390 (2009).
10. Laske, G. *et al.* Asymmetric shallow mantle structure beneath the Hawaiian Swell-evidence from Rayleigh waves recorded by the PLUME network. *Geophys. J. Int.* **187,** 1725–1742 (2011).
11. Rychert, C. *et al.* Seismically imaging destruction of continental lithosphere beneath the Afar and Ethiopian Rift Systems. *Nature Geosci.* **5,** 406–409 (2012).
12. Leahy, G. M., Collins, J. A., Wolfe, C. J., Laske, G. & Solomon, S. C. Underplating of the Hawaiian Swell: Evidence from teleseismic receiver functions. *Geophys. J. Int.* **183,** 313–329 (2010).
13. Stein, C. A. & Stein, S. A model for the global variation in oceanic depth and heat-flow with lithospheric age. *Nature* **359,** 123–129 (1992).
14. Schmerr, N. The Gutenberg discontinuity: Melt at the lithosphere–asthenosphere boundary. *Science* **335,** 1480–1483 (2012).
15. Li, X. *et al.* Mapping the Hawaiian plume conduit with converted seismic waves. *Nature* **405,** 938–941 (2000).
16. Anderson, D. & Sammis, C. Partial melting in the upper mantle. *Phys. Earth Planet. Inter.* **3,** 41–50 (1970).
17. Kawakatsu, H. *et al.* Seismic evidence for sharp lithosphere–asthenosphere boundaries of oceanic plates. *Science* **324,** 499–502 (2009).

18. Rychert, C. A., Rondenay, S. & Fischer, K. M. P-to-S and S-to-P imaging of a sharp lithosphere–asthenosphere boundary beneath eastern North America. *J. Geophys. Res.* **112,** B08314 (2007).
19. Karato, S-I. On the origin of the asthenosphere. *Earth Planet. Sci. Lett.* **321–322,** 95–103 (2012).
20. Hammond, W. C. & Humphreys, E. D. Upper mantle seismic wave velocity: Effects of realistic partial melt geometries. *J. Geophys. Res.* **105,** 10975–10986 (2000).
21. Lee, C. T. A., Luffi, P., Plank, T., Dalton, H. & Leeman, W. P. Constraints on the depths and temperatures of basaltic magma generation on Earth and other terrestrial planets using new thermobarometers for mafic magmas. *Earth Planet. Sci. Lett.* **279,** 20–33 (2009).
22. Bryce, J. G., DePaolo, D. J. & Lassiter, J. C. Geochemical structure of the Hawaiian plume: Sr, Nd, and Os isotopes in the 2.8 km HSDP-2 section of Mauna Kea volcano. *Geochem. Geophys. Geosys.* **6,** Q09G18 (2005).
23. Tarduno, J., Bunge, H-P., Sleep, N. & Hansen, U. The bent Hawaiian-Emperor Hotspot Track: Inheriting the mantle wind. *Science* **324,** 50–53 (2009).
24. Steinberger, B. & Antretter, M. Conduit diameter and buoyant rising speed of mantle plumes: Implications for the motion of hot spots and shape of plume conduits. *Geochem. Geophys. Geosys.* **7,** Q11018 (2006).
25. Cao, Q., van der Hilst, R. D., de Hoop, M. V. & Shim, S. H. Seismic imaging of transition zone discontinuities suggests hot mantle west of Hawaii. *Science* **332,** 1068–1071 (2011).
26. Vidal, V. & Bonneville, A. Variations of the Hawaiian hot spot activity revealed by variations in the magma production rate. *J. Geophys. Res.* **109,** B03104 (2004).
27. Hieronymus, C. F. & Bercovici, D. Discrete alternating hotspot islands formed by interaction of magma transport and lithospheric flexure. *Nature* **397,** 604–607 (1999).
28. Forsyth, D. W. *et al*. Imaging the deep seismic structure beneath a mid-ocean ridge: The MELT experiment. *Science* **280,** 1215–1218 (1998).
29. Hirth, G. & Kohlstedt, D. L. Water in the oceanic upper mantle: Implications for rheology, melt extraction and the evolution of the lithosphere. *Earth Planet. Sci. Lett.* **144,** 93–108 (1996).
30. Faul, U. H. & Jackson, I. The seismological signature of temperature and grain size variations in the upper mantle. *Earth Planet. Sci. Lett.* **234,** 119–134 (2005).

Author contributions

G.L. initiated and deployed the PLUME seismic experiment, calculated station orientations and provided regional expertise and surface wave velocity model. P.M.S. initiated the project and provided reflectivity code for seismic modelling of OBS data. C.A.R. carried out receiver function imaging and modelling and wrote the paper. N.H. carried out geodynamic modelling. C.A.R. and N.H. made figures and developed interpretation. All authors contributed to the manuscript at all stages.

Additional information

The seismic waveforms used in this study are available at the IRIS Data Management Center.

Supplementary information is available in the online version of the paper. Reprints and permissions information is available online at www.nature.com/reprints. Correspondence and requests for materials should be addressed to C.A.R.

Competing financial interests

The authors declare no competing financial interests.